Activation of Autophagy Rescues Amiodarone-Induced Apoptosis of Lung Epithelial Cells and Pulmonary Toxicity in Rats

Kang-Yo Lee,* Sehee Oh,* You-Jin Choi,* Seon-Hee Oh,† Young-Su Yang,‡ Mi-Jin Yang,‡ Kyuhong Lee,‡ and Byung-Hoon Lee*,1

*College of Pharmacy and Research Institute of Pharmaceutical Sciences, Seoul National University, 151-742, Republic of Korea; †Research Center for Oral Disease, Regulation of the Aged, College of Dentistry, Chosun University, Gwangju, 501-759, Republic of Korea; and ‡Inhalation Toxicology Center, Korea Institute of Toxicology, Jeongeup, 580-185, Republic of Korea

1To whom correspondence should be addressed at College of Pharmacy, Seoul National University, Gwanak-ro 1, Gwanak-gu, Seoul 151–742, Republic of Korea. Fax: +82-2-874-7843. E-mail: lee@snu.ac.kr.

   Amiodarone, bi-iodinated benzofuran derivative, is one of the most frequently prescribed and efficacious antiarrhythmic drugs. Despite its low incidence, amiodarone-induced pulmonary toxicity is of great concern and the leading cause of discontinuation. Autophagy is an essential homeostatic process that mediates continuous recycling of intracellular materials when nutrients are scarce. It either leads to a survival advantage or initiates death processes in cells under stress. In the present study, we investigated the role of autophagy in amiodarone-induced pulmonary toxicity. Amiodarone treatment–induced autophagy in H460 human lung epithelial cells and BEAS-2B normal human bronchial epithelial cells was demonstrated by increased LC3-II conversion, *Atg7* upregulation, and autophagosome formation. Autophagic flux, as determined by the lysosomal inhibitor bafilomycin A1, was also increased following amiodarone treatment. To determine the role of autophagy in amiodarone toxicity, amiodarone-induced cell death was evaluated in the presence of 3-methyladenine or by knocking down the autophagy-related genes *Atg7*. Inhibition of autophagy decreased cellular viability and significantly increased apoptosis. Intratracheal instillation of amiodarone in rats increased the number of inflammatory cells recovered from bronchoalveolar lavage fluid, and periodic acid-Schiff-positive staining in bronchiolar epithelial cells. However, induction of autophagy by rapamycin treatment inhibited amiodarone-induced pulmonary toxicity. In conclusion, amiodarone treatment induced autophagy, which is involved in protection against cell death and pulmonary toxicity.

   Key Words: amiodarone; autophagy; apoptosis; pulmonary toxicity.

INTRODUCTION

   Amiodarone is one of the most frequently prescribed and efficacious antiarrhythmic drugs. However, adverse effects in various off-target organs, including cornea, liver, skin, thyroid, and lung, often limit the use of this drug, particularly in the case of long-term treatment. Affected organs share a common feature: accumulation of amiodarone and/or its toxic metabolite (i.e., desethylamiodarone) in the tissue (Wilson and Lippmann, 1990). Both amiodarone and desethylamiodarone tend to accumulate in the lungs due to their amphiphilic nature (Camus and Jeannin, 1984). The incidence of amiodarone-induced pulmonary toxicity (AIPT) is relatively low, yet it is considered to be of great concern and is the leading cause for discontinuation as it can progress into pulmonary fibrosis, an inflammation-driven and life-threatening lung disease with a poor prognosis and no cure (Jessurun and Crijns, 1997). Although the exact mechanisms of AIPT are not fully known, prolonged epithelial cell cytotoxicity provokes cellular immune reactions, which ultimately leads to fibroblast proliferation and collagen deposition (Sheppard and Harrison, 1992). Amiodarone inhibits lysosomal phospholipase activity in the lung, which leads to the induction of pulmonary phospholipidosis (Heath *et al.*, 1985). Even though whether phospholipidosis is related to AIPT remains uncertain, it cannot be ruled out as a contributing factor to this disorder (Camus and Jeannin, 1984).

   Autophagy is an essential homeostatic process that mediates continuous recycling of intracellular materials, such as long-lived proteins and other cellular components, when nutrients are scarce (Lum *et al.*, 2005). Autophagy leads to either a survival advantage or death processes in cells that are under chemical or physiological stress. In some cellular settings, it can serve as a cell-survival pathway, suppressing apoptosis, and in others, it can lead to death itself, either in collaboration with apoptosis or as a backup mechanism when the former is defective (Eisenberg-Lerner *et al.*, 2009). Under many chemical-induced stress conditions, inhibition of autophagy by 3-methyladenine (3-MA) or by knockdown of autophagy-related genes

aggravates chemical toxicity, whereas autophagy induction protects against cell death. In acetaminophen- or ethanol-induced hepatotoxicity, the mechanism by which autophagy protects against tissue injury can be explained by the autophagy-dependent degradation of damaged mitochondria and thus a reduction in the production of reactive oxygen species (ROS; Ding *et al.*, 2010; Ni *et al.*, 2012). Another potential reason why autophagy is cytoprotective is that activated caspase-3 can be degraded by autophagy (Paris *et al.*, 2011).

The mammalian target of rapamycin (mTOR) is a highly conserved serine/threonine kinase that acts as a key regulator of protein synthesis, cell growth, and autophagy in response to cellular nutrient availability and growth factors (Wullschleger *et al.*, 2006). The mTOR inhibits autophagy by phosphorylating proteins involved in autophagosome formation, such as Atg13 and Ulk1, when nutrients are abundant (Kamada *et al.*, 2010). Adenine monophosphate–activated protein kinase (AMPK) is the master regulator of energy metabolism in cells. The energy sensing motif of the enzyme monitors cellular energy status and controls its activity (Hawley *et al.*, 1996). When cells are in need of energy, AMPK shuts down mTOR-mediated anabolic processes and induces autophagy. Class I phosphatidylinositol-3 (PI3) kinases, often activated by growth factors, regulate autophagy via the Akt/mTOR pathway. Growth factor–activated Akt phosphorylates and inhibits the GTPase activity of tuberous sclerosis complex 2, ultimately leading to mTOR activation and inhibition of autophagy (Huang and Manning, 2009). Recently, Balgi *et al.* (2009) reported that amiodarone induces autophagy mediated by mTOR signaling in MCF-7 human breast adenocarcinoma cells. However, they did not elucidate the role of autophagy in AIPT.

In the present study, we assessed the occurrence of autophagy following amiodarone treatment *in vitro* and the relevance of autophagy to *in vivo* pulmonary toxicity. We found that amiodarone activated autophagy in H460 human lung epithelial cells. Suppression of autophagy by 3-MA or siRNA directed at *Atg* aggravated amiodarone toxicity in the cells, whereas induction of autophagy by rapamycin attenuated AIPT in rats.

MATERIALS AND METHODS

Materials. Anti-LC3, anti-p62, anti-Atg5, anti-Atg7, anti-AMPK, anti-phosphor-AMPK (Thr172), anti-Akt, anti-phosphor-Akt (S473), anti-4E-BP1, anti-phosphor-4E-BP1 (S65), anti-p70S6 kinase, anti-phosphor-p70S6 kinase (Thr389), anti-Parp-1, anti-caspase-3, anti-cleaved caspase-3, anti-Bcl-2, anti-β-actin, and anti-GAPDH were purchased from Cell Signaling Technology (Beverly, MA). Anti-GFP was supplied from Santa Cruz Biotechnology (Santa Cruz, CA). Amiodarone hydrochloride, bafilomycin A1 (Baf A1), and 3-MA were obtained from Sigma Chemical Co. (St Louis, MO). Rapamycin was acquired from Enzo Life Sciences (Farmingdale, NY).

Cell culture and amiodarone treatment. H460 human lung epithelial cancer cell line was maintained in RPMI-1640 media (Gibco-BRL, Grand Island, NY) containing 10% heat-inactivated fetal bovine serum (Gibco-BRL) and antibiotics–antimycotics in a 5% CO_2 atmosphere at 37°C. BEGM Bullet Kit (Lonza, Walkersville, MD) was used as culture media for BEAS-2B cells.

Amiodarone was dissolved in methanol at concentrations lower than 0.1% (vol/vol) that do not induce autophagy at least up to 24 h (Supplementary fig. 1). In case of concentration dependency test, same amount of methanol was used throughout the experiments.

Cell viability assay. Cell viability was measured in a 48-well plate in medium containing 10% fetal bovine serum using the 3-(4,5-dimethylthiazol-2-yl)-2,5-diphenyltetrazoliumbromide (MTT) assay. The concentration required for 50% inhibition of growth (IC_{50}) was determined by nonlinear regression analysis using the GraphPad PRISM statistics software package (v. 5.0; San Diego, CA).

Western blot analysis. Cells were washed with PBS and lysed in buffer containing 50mM N-2-hydroxyethylpiperazine-N′-2-ethanesulfonic acid, 150mM sodium chloride, 1% Triton X-100, 5mM ethyleneglycol-bis(aminoethylether)-tetraacetic acid, 50mM glycerophosphate, 20mM sodium fluoride, 1mM sodium orthovanadate, and 2mM PMSF. Cell lysates were then centrifuged, and the protein content was quantified. Equal amounts of protein were separated via SDS-polyacrylamide gel electrophoresis, and these were transferred to a PVDF membrane and probed with specific antibodies. The signal was detected using enhanced chemiluminescence Western blotting detection reagents (Amersham, Piscataway, NJ).

Transient transfection. Adenoviral GFP-LC3B was kindly provided by Dr Xiao-Ming Yin (University of Pittsburgh, Pittsburgh, PA). The siRNA duplexes targeting human Atg7, and nonspecific siRNA, were transfected using Lipofectamine RNAiMAX (Invitrogen, Carlsbad, CA) according to the manufacturer's protocol. Cells were allowed to grow for 30 h following transfection and then treated with amiodarone.

Apoptosis and caspase-3 activity. Cells were stained with Hoechst 33258 and propidium iodide (PI), and visualized under fluorescence microscopy. A minimum of 1000 cells was counted and scored for apoptosis by identifying characteristic chromatin condensation and for necrosis by PI staining. Caspase-3 activity was determined using a CaspACE colorimetric assay system (Promega, Madison, WI) according to the manufacturer's instructions. In brief, the caspase-3 substrate, Ac-DEVD-pNA, was added to cell lysates in assay buffer and monitored with a plate reader at 405 nm.

Transmission electron microscopy. Cells were harvested and fixed with 2% glutaraldehyde in cacodylate buffer (pH 7.2) and postfixed with 1% osmium tetroxide. The cells were dehydrated in increasing concentrations of ethanol and embedded in Spurr's resin. The solidified blocks were cut into thin sections (60 nm) and stained with uranyl acetate and lead citrate for observation with energy-filtered transmission electron microscopy (LIBRA 120; Carl Zeiss, Oberkochen, Germany).

Phospholipid staining. Cells were incubated in medium containing both LipidTox Red Phospholipidosis Detection Reagent (Invitrogen) and amiodarone for 24 h. The cells were fixed with 4% paraformaldehyde and visualized under fluorescence microscope.

Animal experiments. Male F344 rats (10 weeks old) were purchased from Joongang Lab Animal Co. (Seoul, Korea) and housed in an air-conditioned room (24°C) with a 12-h light/dark cycle. After a 1-week adaptation period, the animals were divided into four groups. The control group received a vehicle by intratracheal (i.t.) instillation. The rapamycin group was given rapamycin (4 mg/kg; ip) 30 min prior to vehicle administration. Rats in the amiodarone group were administered amiodarone (6.25 mg/kg; i.t.). The rapamycin and amiodarone group received rapamycin 30 min before amiodarone administration. Amiodarone was dosed twice at days 1 and 3, whereas rapamycin was injected four times on days 1, 2, 3, and 4. Rats were killed 1 h after the final rapamycin treatment. Animal experiments were carried out in accordance with animal experiment guidelines and with approval of the Animal Care and Use Committee of the institute.

Histology. The lungs were fixed in 4% paraformaldehyde and embedded in paraffin. Sections were cut and stained with periodic acid-Schiff (PAS).

Bronchoalveolar lavage. Bronchoalveolar lavage (BAL) was performed on day 4. The rats were anesthetized and exsanguinated by severing the abdominal aorta. The left bronchus was clamped off, and BAL was performed on the right lung three times using separate 3-ml aliquots of warm, calcium-free and magnesium-free PBS (pH 7.4). Measurements of the total and differential counts in BAL fluid (BALF) cells were also performed as described previously (Yang *et al.*, 2008).

Immunohistochemistry. Immunohistochemical staining was performed using rabbit anti-LC3A monoclonal antibody. Sections were counterstained with meyer's hematoxylin.

Statistical analysis. All data are expressed as the mean ± SD of at least three independent experiments. Statistical analysis was performed using a one-way ANOVA followed by Tukey's *post hoc* test. Differences between groups were considered to be statistically significant at $p < 0.05$.
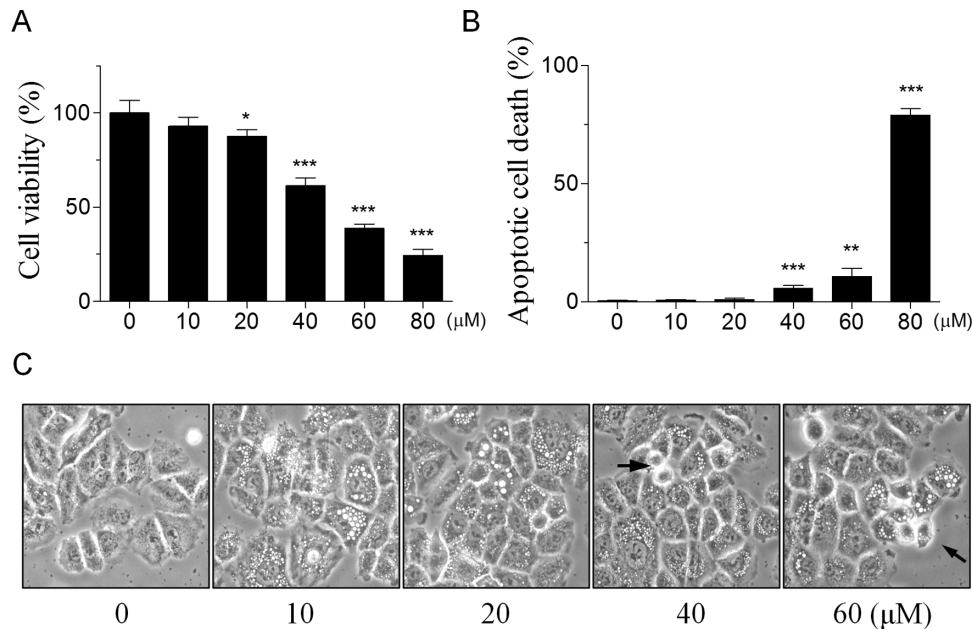
RESULTS

Amiodarone Treatment Induces Apoptotic Cell Death in H460 Cells

When H460 cells were incubated with amiodarone-containing media for 24 h and cellular viability was determined by MTT assay, the amiodarone concentration that induced the half-maximal effect (IC_{50}) was calculated as 46.0µM (Fig. 1A). IC_{50} for BEAS-2B cells were 4.4µM. Apoptotic death of H460 cells was measured by fluorescence microscopy following PI staining. The number of apoptotic cells increased beginning at 40µM concentration. Approximately 80% of cells underwent apoptosis following treatment with 80µM amiodarone (Fig. 1B). As shown in Figure 1C, amiodarone treatment caused morphological changes in H460 cells. Increased numbers of cytoplasmic vacuoles are prominent at lower concentration of amiodarone, whereas round and floating cells were observed as the amiodarone concentration increased.

Amiodarone Inhibits mTOR Signaling Pathway and Induces Autophagy

We tested whether amiodarone induces autophagy in H460 and BEAS-2B cells by determining the conversion of cytoplasmic LC3-I into autophagosome membrane-bound LC3-II; the expression of Atg5 and Atg7, essential proteins for autophagosome formation (Levine and Klionsky, 2004); and the degradation of p62, an autophagy-specific substrate (Komatsu *et al.*, 2007). Western blot analysis showed a concentration- and time-dependent increase in LC3-II and Atg7 in amiodarone-treated cells. The level of p62 does not decrease with the induction of autophagy probably due to the lysosomotropic effect of amiodarone (Figs. 2A and 2B; Supplementary figs. 2A and 2B). More details on the discrepancy are described in the Discussion section. LC3-II conversion by amiodarone was also investigated using fluorescence microscopy following transient transfection with GFP-LC3. As shown in Figure 2C, diffuse GFP-LC3 cytoplasmic staining was observed in untreated control cells, whereas amiodarone-treated cells had LC3-positive GFP puncta. The GFP-LC3 puncta do not colocalize to the cytoplasmic vacuoles indicating that the amiodarone-induced vacuoles have little to do with autophagy (Supplementary fig. 3A). We also analyzed the cellular ultrastructure by electron microscopy to confirm that autophagy was induced by amiodarone.

FIG. 1. Amiodarone induces apoptotic cell death in H460 cells. Cells were incubated with the indicated amiodarone concentrations. Cell viability was determined by MTT assay at 24 h (A) and apoptosis was evaluated using PI staining at 21 h (B). (C) Representative photomicrographs (×400) of cells treated with amiodarone for 6 h show formation of cytoplasmic vacuoles. Round and floating cells are seen at higher concentrations (arrows). The data are expressed as the mean ± SD of results obtained from three independent experiments. *$p < 0.05$, **$p < 0.01$, ***$p < 0.001$ compared with the control.
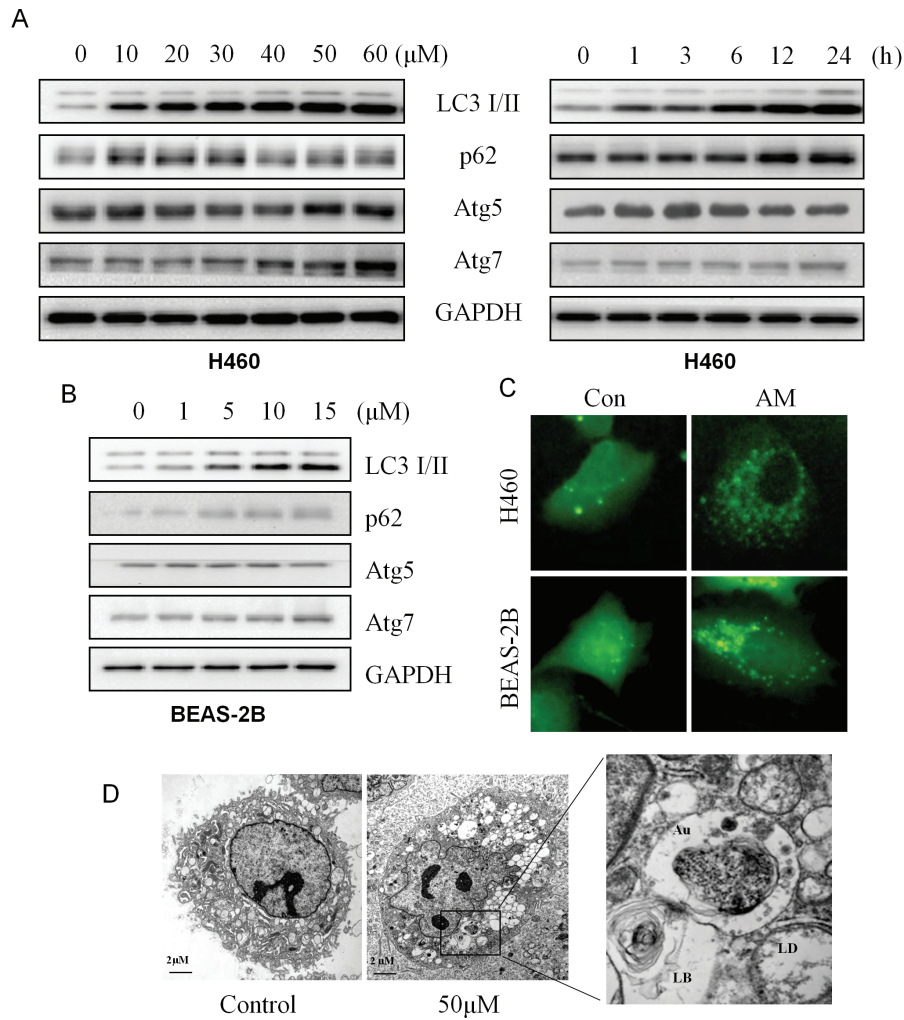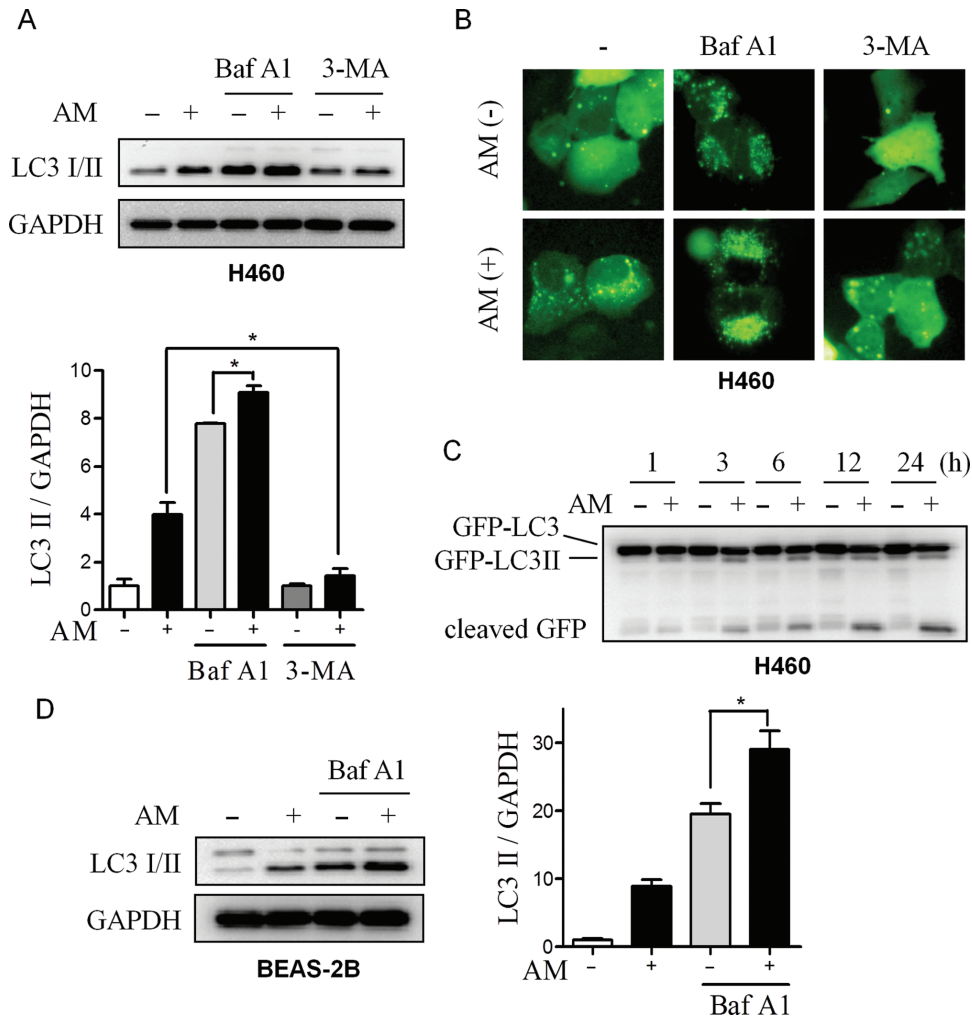
FIG. 2. Amiodarone induces autophagy in H460 and BEAS-2B cells. H460 cells were treated with amiodarone as indicated, and Western blot analysis was performed using specific antibodies to examine protein expression in whole cell lysates. Representative photomicrographs (×400) from more than three independent experiments are shown (A). BEAS-2B cells were treated with amiodarone as indicated, and Western blot analysis was performed (B). Cells were transfected with the GFP-LC3 plasmid for 6h and then incubated with amiodarone for another 6h before analysis by fluorescence microscopy. Representative images of GFP-LC3 staining with or without amiodarone treatment are shown (×400) (C). Representative electron micrographs of cells incubated with 50 µM amiodarone for 18 h are shown (D).

Amiodarone treatment led to the formation of numerous lipid droplets, shown as hollow cytoplasmic vesicles and lamellar bodies, a hallmark of phospholipidosis. Furthermore, autophagosome containing cytoplasmic components were observed in amiodarone-treated cells (Fig. 2D).

We next assessed autophagic flux using the lysosomal inhibitor Baf A1. The optimal concentration of Baf A1 was determined as shown in Supplementary figure 4A. Treatment of H460 cells with Baf A1 alone increased the LC3-II level and GFP-LC3 puncta in the absence of amiodarone, indicating lysosomal inhibition and autophagosome accumulation. LC3-II conversion and GFP-LC3 puncta further increased in the presence of Baf A1 following amiodarone treatment. In contrast, cells pretreated with 3-MA, an autophagic sequestration inhibitor, exhibited reduced LC3-II conversion and GFP-LC3 puncta by amiodarone compared with nonpretreated cells (Figs. 3A and 3B). Autophagic flux was also determined by detecting free GFP fragment formed by degradation of GFP-LC3 in autophagolysosome. Amiodarone treatment increased GFP generation in time- and concentration-dependent manner (Fig. 3C; Supplementary fig. 4B). However, amiodarone-induced free GFP was significantly reduced in Baf A1 pretreated cells (Supplementary fig. 4C). Similar results were observed in BEAS-2B cells treated with amiodarone (Fig. 3D; Supplementary figs. 4B and 4C). Finally autophagic flux was also monitored by detecting autophagosome-lysosome fusion. H460 cells were transfected with GFP-LC3, incubated with amiodarone and stained with Lysotracker Red. As shown in Supplementary figure 5, red fluorescence overlapped with GFP-LC3 in amiodarone-treated cells indicating the delivery of autophagosome to lysosome. These

FIG. 3. Amiodarone increases autophagic flux in H460 and BEAS-2B cells. Cells were pretreated with Baf A1 (150nM for H460 and 50nM for BEAS-2B) or 3-MA (10mM) for 1 h and then incubated with amiodarone (50μM for H460; 15μM for BEAS-2B) for another 4 h. Western blot analysis was used to examine LC3 I/II expression in H460 cells (A) and BEAS-2B (D) cells, and densitometric analysis was performed. H460 cells were transfected with GFP-LC3 as described in Figure 1. Cells were preincubated Baf A1 or 3-MA for 1 h and then incubated with 50μM of amiodarone and visualized with fluorescence microscope (B). H460 cells were transfected with GFP-LC3 and incubated with amiodarone for indicated time. Western blot analysis was performed using antibodies against GFP (C). *$p < 0.05$ compared with the corresponding group.

data clearly demonstrate that amiodarone induces autophagy in H460 and BEAS-2B cells.

The mTOR regulates protein synthesis and cell growth by sensing cellular nutrient status. AMPK activation or Akt inhibition blocks the mTOR signal cascade and leads to apoptosis. Starvation induces autophagy in MCF-7 cells through mTOR inhibition. Therefore, chemicals that inhibit mTOR activity via AMPK activation or Akt inhibition also induce autophagy. Amiodarone was recently reported to induce autophagy in eukaryotic cells by inhibiting mTORC1 signaling (Balgi *et al.*, 2009). AMPK phosphorylation at Thr172 was increased, and Akt phosphorylation at Ser473 was decreased by amiodarone treatment, which resulted in attenuated mTOR activity as determined by the reduced phosphorylation levels of p70S6 kinase and 4E-BP (Figs. 4A and 4B; Supplementary figs.

6A and 6B). The mTOR signaling pathway was also induced in BEAS-2B cells (Fig. 4C).

Amiodarone-Induced Autophagy Protects H460 Cells from Apoptosis

Next, we asked whether amiodarone-induced autophagy affects the life and death of the cells by determining cell viability and apoptotic cell death in the absence or presence of 3-MA. Inhibition of basal autophagy by 3-MA decreased cellular viability and increased apoptosis slightly but significantly. Treatment of cells with amiodarone in the presence of 3-MA led to a 72% decrease in cell viability compared to treatment with amiodarone alone, in which a 30% decrease in cell viability was observed (Fig. 5A). Similarly, apoptotic cell number was markedly increased in the co-treatment group (Figs. 5B and 5C).
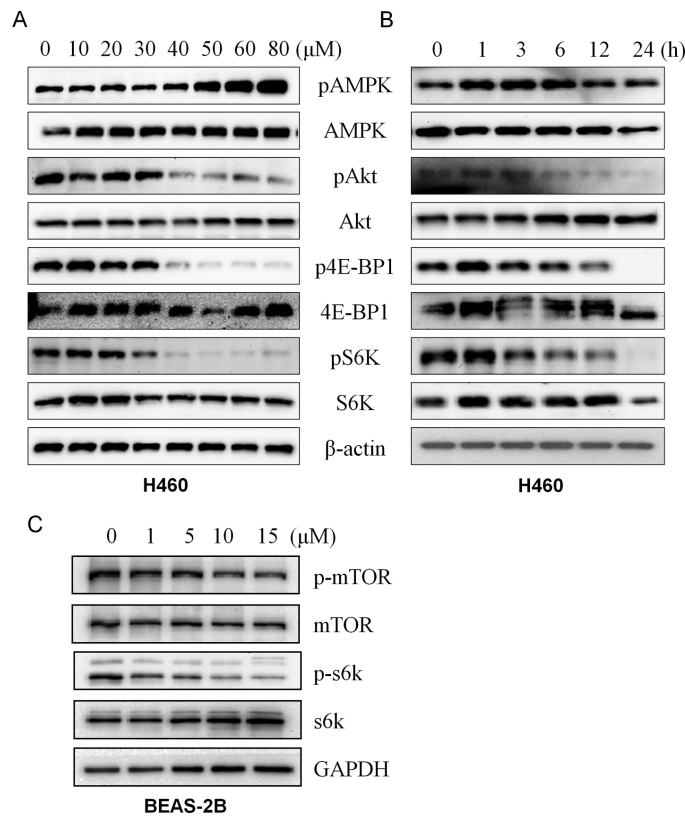
FIG. 4. Amiodarone induces AMPK- and Akt-mediated mTOR-dependent autophagy. H460 (A and B) and BEAS-2B (C) cells were incubated with amiodarone as indicated, and Western blot analysis using specific antibodies was performed to examine protein expression in whole cell lysates. Representative images from more than three independent experiments are shown.
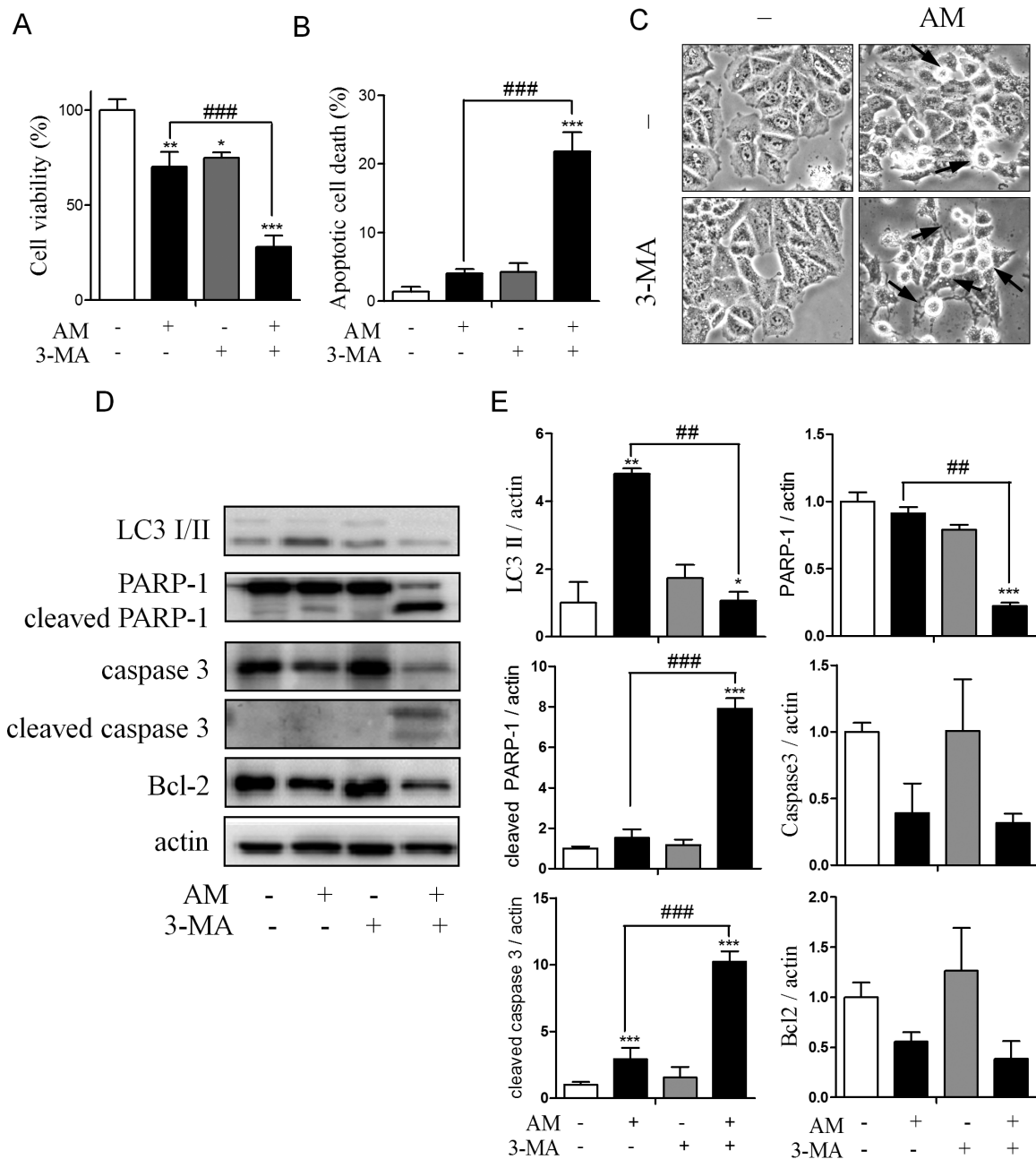
Inhibition of autophagy in 3-MA/amiodarone co-treated cells was confirmed by reduced LC3-II. Under this condition, PARP and caspase-3 cleavage were observed in cells, both of which are positive regulators of apoptotic cell death. Compared with the amiodarone-treated group, 3-MA co-treatment significantly reduced the expression of anti-apoptotic Bcl-2 (Figs. 5D and 5E).

To further investigate the role of autophagy in amiodarone cytotoxicity, *Atg7*-specific siRNA was transfected into H460 cells. Transfection of siRNA against *Atg7* decreased the amiodarone-induced cell viability and increased apoptosis and caspase-3 activity induced by amiodarone (Figs. 6A–C). Inhibition of autophagy by knocking down autophagy-related genes completely blocked amiodarone-induced autophagy as determined by LC3-II levels (Figs. 6D and 6E). Apoptosis induction was further corroborated by Western blot analysis. Amiodarone treatment in the siRNA-transfected cells increased caspase-3 cleavage and decreased anti-apoptotic Bcl-2 expression (Figs. 6D and 6E). These results clearly indicate that inhibition of autophagy sensitizes H460 cells to amiodarone-induced cytotoxicity and apoptosis.

Autophagy Protects Rats from AIPT

To investigate the role of autophagy in AIPT, rats were administered amiodarone by intratracheal instillation with or without rapamycin. The animal models for AIPT develop inflammatory and fibrotic reaction similar to that observed in AIPT patients (Chung *et al.*, 2001; Reinhart and Gairola, 1997; Taylor *et al.*, 2000). High-performance liquid chromatography analysis revealed that amiodarone concentration of 497.3 ± 259.1 ng/g lung tissue was much lower than that observed in the AIPT patient (Brien *et al.*, 1987). We performed BALF total and differential cell counts as a marker of airway inflammation. The number of neutrophils and eosinophils was significantly elevated by amiodarone treatment, which was significantly inhibited by rapamycin. The number of macrophages was also increased by amiodarone by twofold, although statistically not significant. Consequently, amiodarone treatment increased the total BAL cell count by fourfold; however, co-treatment with rapamycin decreased the number significantly (Fig. 7A). Goblet cells, which are situated in the epithelium, contribute to a rapid response to airborne irritants, particles, and micro-organisms (Rogers, 2003). Increased goblet cell number and mucin secretion are characteristic features of chronic bronchitis (Saetta *et al.*, 2000) and cystic fibrosis (Burgel *et al.*, 2007). PAS staining showed minimal positive staining in control and rapamycin groups, whereas amiodarone administered rats showed significant magenta staining. However, co-treatment with rapamycin completely attenuated the number of PAS-positive cells. Furthermore, amiodarone-induced goblet cell hyperplasia occurred in the bronchioles was blocked by the pretreatment with rapamycin
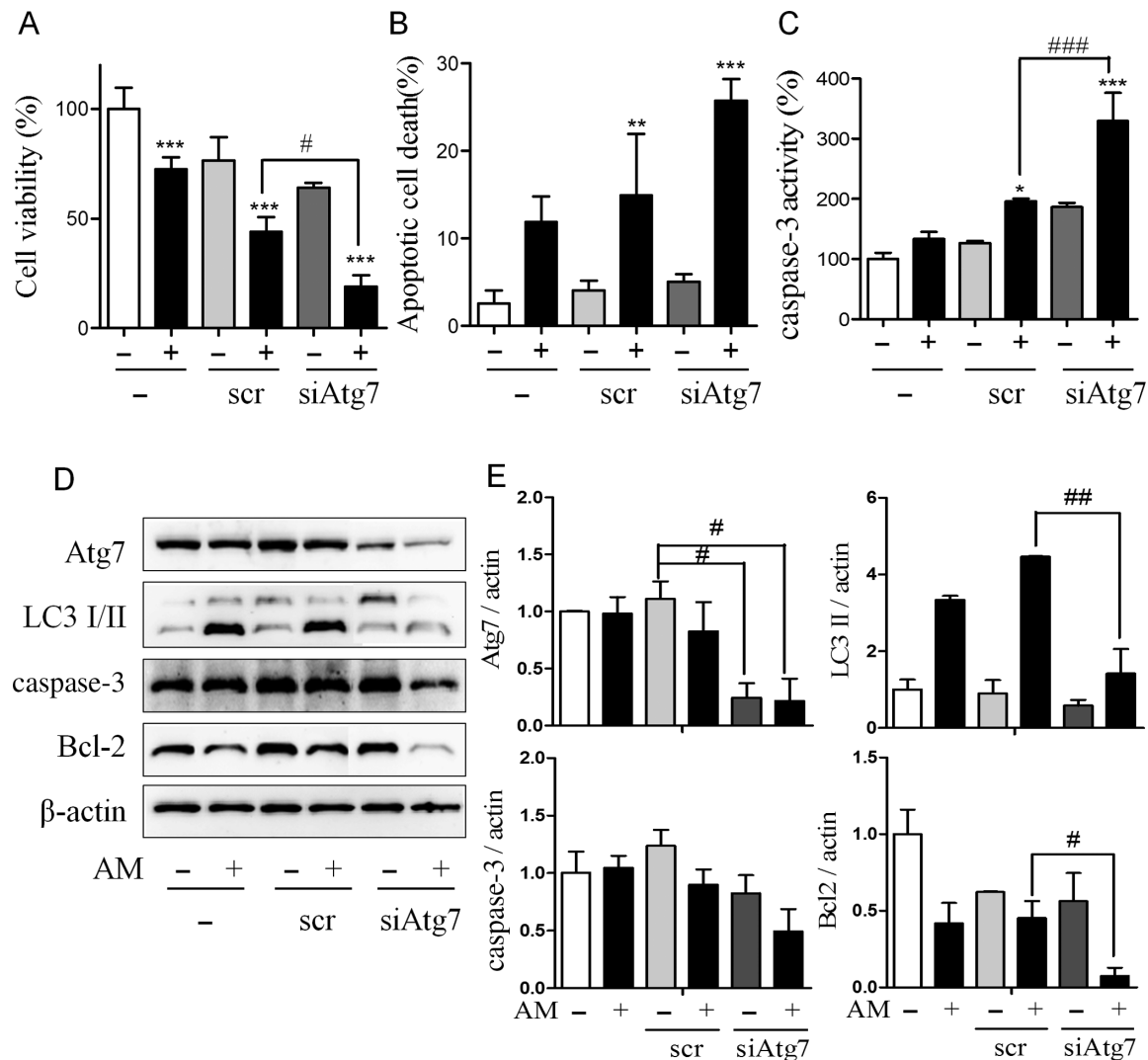
FIG. 5. Inhibition of autophagy by 3-MA increases the susceptibility of H460 cells to amiodarone cytotoxicity. Cells were incubated with 50 μM amiodarone for 21 h following 1 h pretreatment with or without 10 mM 3-MA. Cell viability (A) and apoptosis (B) were evaluated as described in Figure 1. Representative photomicrographs ($\times$400) of cells treated with amiodarone for 6 h show an increased number of floating cells (arrow) in the presence of 3-MA (C). Western blot analysis using specific antibodies was performed to examine protein expression in whole cell lysates. Representative images from more than three independent experiments are shown (D) and densitometric analysis was performed (E). The data are expressed as the mean ± standard deviation (SD) of results obtained from three independent experiments. *$p < 0.05$, **$p < 0.01$, ***$p < 0.001$ compared with the control, ##$p < 0.01$ ###$p < 0.001$ compared with the amiodarone group.

(Fig. 7B). Immunohistochemical staining of the lung tissue demonstrates that the expression of LC3A was notably increased in the bronchial epithelial cells of rapamycin, as well as rapamycin and amiodarone-treated rats (Fig. 7C). Overall, our results demonstrate that rapamycin-activated autophagy rescued mucin secretion, goblet cell hyperplasia, and airway inflammation induced by amiodarone.

DISCUSSION

Amiodarone is one of the most frequently prescribed antiarrhythmic drugs, but pulmonary toxicity seen in patients following long-term treatment is often the cause of discontinuation. Amiodarone was recently reported to induce autophagy mediated by mTOR activation in human breast

FIG. 6. Inhibition of autophagy by siRNA against *Atg7* gene increases the susceptibility of H460 cells to amiodarone cytotoxicity. Cells were transfected with scrambled control siRNA or siRNA against *Atg7* and treated with 50μM amiodarone for 18 h, and viability (A), apoptosis (B), and caspase-3 activity (C) were examined. $*p < 0.05$, $**p < 0.01$, $***p < 0.001$ compared with the control, $^\#p < 0.05$, $^{\#\#\#}p < 0.001$ compared with the amiodarone group transfected with scrambled control siRNA. Western blot analysis using specific antibodies was performed to examine protein expression in whole cell lysates. Representative images from more than three independent experiments are shown (D), and densitometric analysis was performed (E). The data are expressed as the mean ± SD of results obtained from three independent experiments. $^\#p < 0.05$, $^{\#\#}p < 0.01$ compared with the corresponding group transfected with scrambled control siRNA.

cancer cells (Balgi *et al.*, 2009). Amiodarone accumulates in intracellular vacuoles, which are positive for autophagy markers, in HEK 293 cells and in tissue obtained from a patient biopsy of amiodarone-induced blue-gray skin discoloration (Morissette *et al.*, 2009). Although amiodarone is reportedly an autophagy inducer, much less evidence and understanding is currently available regarding the role of autophagy in amiodarone toxicity. Amiodarone induces mitochondrial damage, leading to ROS production (Serviddio *et al.*, 2011). ROS cause various cellular damage that can be attenuated by antioxidant responses, including autophagy.

In the present study, we hypothesized that amiodarone-induced autophagy is a protective mechanism against cytotoxicity and thus that AIPT can be prevented by the

activation of autophagy. To test this hypothesis, we investigated amiodarone-induced autophagy and the role of autophagy in amiodarone-induced cell death by analyzing autophagy-specific molecular and cellular markers in H460 human lung epithelial cells and BEAS-2B normal human bronchial epithelial cells, the latter of which are reported to possess similar characteristic with primary bronchial cells in terms of autophagy (Chen *et al.*, 2008). Amiodarone increased LC3-II and Atg7, as well as autophagic flux. Inhibition of autophagy decreased cellular viability and significantly increased apoptosis. We also investigated the effects of autophagy on pulmonary toxicity in rats administered amiodarone. In line with previous findings, amiodarone induced autophagy mediated by mTOR inhibition in H460 human lung epithelial cells. This study is the first to
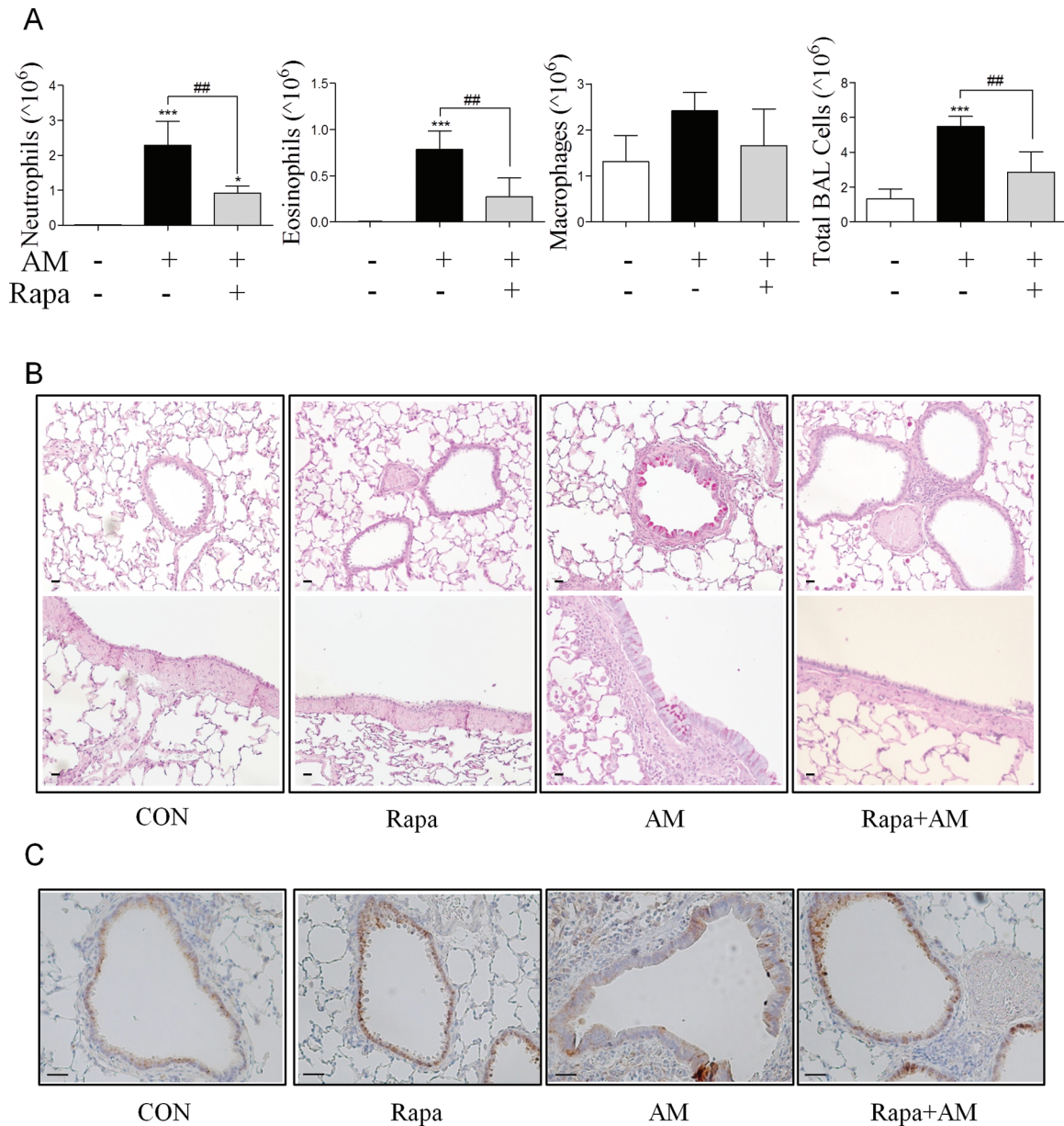
FIG. 7. Activation of autophagy by rapamycin protects lungs from amiodarone-induced pulmonary toxicity. Rats were instilled with vehicle (CON) or amiodarone (AM) and rapamycin (Rapa) was injected 30 min prior to amiodarone administration. On day 4, rats were anesthetized, and BAL and total and differential cell count were performed (A). Fixed lung sections were subjected to immunohistochemistry using antibody against LC3A (B) and PAS staining (C). Representative microphotographs of lung specimens from all groups are shown. $*p < 0.05$, $***p < 0.001$ compared with the control, $^{\#\#}p < 0.01$ compared with the amiodarone group. Scale bars: 100 µm.

demonstrate that suppression of autophagy aggravated the cytotoxicity of amiodarone in H460 cells, whereas induction of autophagy attenuated amiodarone-induced mucus oversecretion and goblet cell hyperplasia in the rat lung. These results clearly indicate that autophagy is a protective mechanism against AIPT.

The level of p62 did not decrease with the induction of autophagy. The number of cytoplasmic vacuoles did not match with the degree of autophagy as well. The reason for the discrepancies can be explained by the lysosomotropic effect of amiodarone leading to the impairment of lysosomal function

and phospholipid metabolism. Amiodarone-induced formation of intracytoplasmic inclusions was also reported in bovine pulmonary artery endothelial cells (Martin and Howard, 1985). As the nature of the vacuole, they suggested lamellar structure, which has been previously described as characteristic of phospholipid formation (Lullman *et al.*, 1975) and have also been described *in vivo* amiodarone toxicity (Marchlinski *et al.*, 1982). We demonstrated that amiodarone-induced vacuoles do not colocalize to GFP-LC3 ruling out the possibility of autophagic vacuoles (Supplementary fig. 3A). Moreover,

the dose-response pattern of vacuole formation and accumulation of phospholipid are very similar (Supplementary fig. 3B). Therefore, we suggest that amiodarone-induced vacuoles have little to do with autophagy but with phospholipidosis. As a result, impairment of lysosomal function by amiodarone may disturb lysosomal degradation of autophagic substrate including p62. In spite of all these changes, high-dose amiodarone-induced autophagy is evident as shown in the concentration-dependent increase in the autophagic flux and autophagosome turnover. Therefore, we suggest that amiodarone at lower concentrations induces both autophagy and lysosomal impairment that are somewhat balanced. When the concentration of amiodarone increases, however, autophagy becomes dominant over the lysosomal effect. Several other mechanisms including proteasomal degradation and oxidative stress cannot be ruled out as possible explanation of the discrepancy (Jain et al., 2010).

Endoplasmic reticulum (ER) stress can trigger autophagy to degrade misfolded proteins and to protect against ER stress-induced apoptosis (Ogata et al., 2006). For example, aminochrome induces cell death in a cell line derived from rat substantia nigra through caspase-3 activation, cytochrome c release, and mitochondrial damage, and leads to a significant increase in the number of autophagic vacuoles. When cells were incubated with an autophagy inhibitor, the number of apoptotic cells was increased, whereas preincubation with rapamycin significantly decreased cell death due to the autophagy-mediated degradation of damaged mitochondria and recycling through lysosomes (Paris et al., 2011). Similarly, activation of autophagy by rapamycin has protective role against acetaminophen-induced hepatotoxicity (Ni et al., 2012) and reduces neurodegeneration in a fly and mouse model (Ravikumar et al., 2004). Moreover, autophagy plays a self-protective role against arsenic-induced cell transformation, an important step in arsenic tumorigenesis (Zhang et al., 2012).

Akt is a survival factor that promotes cell proliferation; thus, a defective Akt pathway is found in many types of cancer. Acute ER stress results in suppression of the Akt/TSC/mTOR signaling pathway, which contributes to ER stress-induced autophagy (Qin et al., 2010). Amiodarone inhibits diverse ion channels, including the Na^+/Ca^{2+} exchanger, Ca^{2+} channels, and Na^+ channels (Kodama et al., 1999). Because the Na^+/Ca^{2+} exchanger is one of the most important cellular mechanisms involved in removing the cellular Ca^{2+} ion, inhibition of the transporter by amiodarone increases intracellular Ca^{2+} and Ca^{2+} signaling in various cell types (Powis et al., 1990). Increased levels of intracellular Ca^{2+} lead to ER stress (Tsutsumi et al., 2006). Considering that amiodarone leads to increased Ca^{2+} due to its action as an ion channel inhibitor and the role of Ca^{2+} in ER stress, it is not surprising that amiodarone induces ER stress. According to our data (Supplementary fig. 7) and those from others (Kim et al., 2011), amiodarone increases the expression and phosphorylation of ER stress-associated proteins, including C/EBP homologous protein, inositol-requiring protein-1,

RNA-activated protein-kinase-like ER kinase, and eukaryotic translation initiation factor 2. Therefore, we postulate that amiodarone-induced autophagy can be initiated by the activation of ER stress in response to intracellular Ca^{2+} influx and executed by ER-stress-induced inhibition of PI3 kinase and subsequent decrease in Akt phosphorylation and mTOR activity (Fig. 4; Supplementary fig. 7).

Autophagy-associated genes are under the control of mTOR, and the inhibition of mTOR by rapamycin treatment enhances autophagy (Floto et al., 2007; Rosenbluth and Pietenpol, 2009). Another explanation for reduced Akt phosphorylation by amiodarone can be deduced from the fact that AIPT is initiated by mitochondrial dysfunction and ROS (Bolt et al., 2001). ROS impair the Akt/mTOR pathway, ultimately leading to apoptotic and autophagic cell death. Incubation of U251 cells with H_2O_2 leads to changes in mitochondrial permeability in association with decreased Akt phosphorylation and mTOR activity (Zhang et al., 2009). Moreover, ROS increase AMPK phosphorylation as a result of the increased AMP:ATP ratio, as well as tyrosine kinase activity independent of the cellular adenosine nucleotide levels (Choi et al., 2001). AMPK activation negatively regulates mTOR activity and thus induces autophagy. Given the positive and negative regulatory roles of AMPK and Akt in mTOR activity, respectively, it is not surprising that amiodarone induces autophagy mediated by Akt/mTOR and AMPK/mTOR signaling axes (Fig. 4). Cross talk between the axes is not clear and requires further investigation.

The mechanisms by which autophagy acts to attenuate apoptosis are not fully understood, but recent studies provide some clues. In eukaryotes, mitochondria are not only the site of aerobic energy production, but also for ROS production. Moreover, defective mitochondria accelerate the production of ROS that attack nucleic acids. Therefore, activation of autophagy for timely elimination of aged and dysfunctional mitochondria is essential to protect cells from disordered mitochondrial metabolism (Kim et al., 2007). Disruption of mitochondrial function and cellular ATP levels are initial events in AIPT (Bolt et al., 2001). Note that ROS scavengers, such as ubiquinone and α-tocopherol, effectively protect lung epithelial cells from amiodarone-induced toxicity (Nicolescu et al., 2008). These results indicate that the disposal of damaged mitochondria, or at least excess ROS, confers cells with resistance to chemical stress. Possible mechanisms by which activation of autophagy protects from AIPT can be explained in this regard.

Patients with AIPT are characterized by eosinophilic pneumonia, interstitial pneumonitis, bronchiolitis obliterans organizing pneumonia (BOOP), and fibrosis. For the study of AIPT, animal models have been developed and characterized in rats by intratracheal instillation of amiodarone (Reinhart et al., 1996; Reinhart and Gairola, 1997; Taylor et al., 2000). Direct accumulation of amiodarone in lung tissue leads to an inflammatory and fibrotic reactions similar to those observed in AIPT patients. Representative changes observed in the model include acute inflammation revealed by total and differential

cells recovered by BALF, interstitial pneumonia, and alveolar thickening. Moreover, acute exposure of amiodarone induces pulmonary fibrosis within 6 weeks, which is very relevant to human AIPT (Reinhart *et al.*, 1996; Taylor *et al.*, 2000). We used the same model of Taylor *et al.*, (2000) and found similar changes such as increased neutrophils and eosinophils in BALF, as well as alveolar thickening and granulomatous inflammation in PAS staining.

Goblet cells, situated in the epithelium of conducting airways, secrete high-molecular-weight mucus glycoproteins (mucins) and act as a first-line defender against airborne irritants, particles, and micro-organisms (Rogers, 2003) via a process called mucociliary clearance. Mucus overproduction impairs mucociliary clearance and may contribute to the development of chronic inflammation and bacterial colonization seen in cystic fibrosis patients (Ramsey, 1996). Therefore, it is important to maintain mucus quality and quantity. Intratracheal instillation of amiodarone induced PAS-positive staining and goblet cell hyperplasia, whereas co-treatment with rapamycin activated autophagy and inhibited mucus overproduction and goblet cell hyperplasia. As inflammatory cells are increasingly recruited in the lung, they can release a variety of inflammatory mediators and ROS that can lead to chronic inflammation and fibrosis development. Activation of autophagy with rapamycin decreased pulmonary inflammation by decreasing BALF total cells and differential cells, which were increased by amiodarone administration. Although the effect of rapamycin might be somewhat attributed to the immunosuppressive property, there are many evidences that enhanced autophagy by rapamycin reduces pulmonary toxicity (Abdulrahman *et al.*, 2011; Yen *et al.*, 2013). Moreover, we demonstrated that in rats administered with rapamycin, LC3A expression was significantly increased in the bronchial epithelial cells (Fig. 7C). These results indicate that decreased pulmonary inflammation and goblet cell hyperplasia by increased autophagy can protect against AIPT.

In summary, this study highlights the role of autophagy in AIPT in rats. Amiodarone induced AMPK and Akt-mediated inhibition of mTOR and autophagy, which functions to rescue stressed cells from apoptotic cell death. Consequently, induction of autophagy by rapamycin administration attenuated AIPT in rats.

SUPPLEMENTARY DATA

Supplementary data are available online at http://toxsci. oxfordjournals.org/.

FUNDING

REFERENCES

Abdulrahman, B. A., Khweek, A. A., Akhter, A., Caution, K., Kotrange, S., Abdelaziz, D. H., Newland, C., Rosales-Reyes, R., Kopp, B., McCoy, K., *et al.* (2011). Autophagy stimulation by rapamycin suppresses lung inflammation and infection by Burkholderia cenocepacia in a model of cystic fibrosis. *Autophagy* **7,** 1359–1370.

Balgi, A. D., Fonseca, B. D., Donohue, E., Tsang, T. C., Lajoie, P., Proud, C. G., Nabi, I. R., and Roberge, M. (2009). Screen for chemical modulators of autophagy reveals novel therapeutic inhibitors of mTORC1 signaling. *PLoS One* **4,** e7124.

Bolt, M. W., Card, J. W., Racz, W. J., Brien, J. F., and Massey, T. E. (2001). Disruption of mitochondrial function and cellular ATP levels by amiodarone and N-desethylamiodarone in initiation of amiodarone-induced pulmonary cytotoxicity. *J. Pharmacol. Exp. Ther*. **298,** 1280–1289.

Brien, J. F., Jimmo, S., Brennan, F. J., Ford, S. E., and Armstrong, P. W. (1987). Distribution of amiodarone and its metabolite, desethylamiodarone, in human tissues. *Can. J. Physiol. Pharmacol*. **65,** 360–364.

Burgel, P. R., Montani, D., Danel, C., Dusser, D. J., and Nadel, J. A. (2007). A morphometric study of mucins and small airway plugging in cystic fibrosis. *Thorax* **62,** 153–161.

Camus, P., and Jeannin, L. (1984). Re: Speculation on the mechanism for amiodarone-induced pneumonitis. *Radiology* **150,** 279–280.

Chen, Z. H., Kim, H. P., Sciurba, F. C., Lee, S. J., Feghali-Bostwick, C., Stolz, D. B., Dhir, R., Landreneau, R. J., Schuchert, M. J., Yousem, S. A., *et al.* (2008). Egr-1 regulates autophagy in cigarette smoke-induced chronic obstructive pulmonary disease. *PLoS One* **3,** e3316.

Choi, S. L., Kim, S. J., Lee, K. T., Kim, J., Mu, J., Birnbaum, M. J., Soo Kim, S., and Ha, J. (2001). The regulation of AMP-activated protein kinase by H(2)O(2). *Biochem. Biophys. Res. Commun*. **287,** 92–97.

Chung, W. H., Bennett, B. M., Racz, W. J., Brien, J. F., and Massey, T. E. (2001). Induction of c-jun and TGF- in Fischer 344rats during amiodarone-induced pulmonary fibrosis. *Am. J. Physiol. Lung Cell Mol. Physiol*. **281,** 1180–1188.

Ding, W. X., Li, M., Chen, X., Ni, H. M., Lin, C. W., Gao, W., Lu, B., Stolz, D. B., Clemens, D. L., and Yin, X. M. (2010). Autophagy reduces acute ethanol-induced hepatotoxicity and steatosis in mice. *Gastroenterology* **139,** 1740–1752.

Eisenberg-Lerner, A., Bialik, S., Simon, H-U., Kimchi, A., (2009). Life and death partner: apoptosis, autophagy and the cross-talk between them. *Cell Death Diff*. **16,** 966–975.

Floto, R. A., Sarkar, S., Perlstein, E. O., Kampmann, B., Schreiber, S. L., and Rubinsztein, D. C. (2007). Small molecule enhancers of rapamycin-induced TOR inhibition promote autophagy, reduce toxicity in Huntington's disease models and enhance killing of mycobacteria by macrophages. *Autophagy* **3,** 620–622.

Hawley, S. A., Davison, M., Woods, A., Davies, S. P., Beri, R. K., Carling, D., and Hardie, D. G. (1996). Characterization of the AMP-activated protein kinase kinase from rat liver and identification of threonine 172 as the major site at which it phosphorylates AMP-activated protein kinase. *J. Biol. Chem*. **271,** 27879–27887.

Heath, M. F., Costa-Jussà, F. R., Jacobs, J. M., and Jacobson, W. (1985). The induction of pulmonary phospholipidosis and the inhibition of lysosomal phospholipases by amiodarone. *Br. J. Exp. Pathol*. **66,** 391–397.

Huang, J., and Manning, B. D. (2009). A complex interplay between Akt, TSC2 and the two mTOR complexes. *Biochem. Soc. Trans*. **37**(Pt 1), 217–222.

Jain, A., Lamark, T., Sjøttem, E., Larsen, K. B., Awuh, J. A., Øvervatn, A., McMahon, M., Hayes, J. D., and Johansen, T. (2010). p62/SQSTM1 is a target gene for transcription factor NRF2 and creates a positive feedback loop by inducing antioxidant response element-driven gene transcription. *J. Biol. Chem*. **285,** 22576–22591.

Jessurun, G. A., and Crijns, H. J. (1997). Amiodarone pulmonary toxicity. *BMJ* **314,** 619–620.

Kamada, Y., Yoshino, K., Kondo, C., Kawamata, T., Oshiro, N., Yonezawa, K., and Ohsumi, Y. (2010). Tor directly controls the Atg1 kinase complex to regulate autophagy. *Mol. Cell. Biol.* **30,** 1049–1058.

Kim, I., Rodriguez-Enriquez, S., and Lemasters, J. J. (2007). Selective degradation of mitochondria by mitophagy. *Arch. Biochem. Biophys.* **462,** 245–253.

Kim, I. Y., Kang, Y. J., Yoon, M. J., Kim, E. H., Kim, S. U., Kwon, T. K., Kim, I. A., and Choi, K. S. (2011). Amiodarone sensitizes human glioma cells but not astrocytes to TRAIL-induced apoptosis via CHOP-mediated DR5 upregulation. *Neuro. Oncol.* **13,** 267–279.

Kodama, I., Kamiya, K., and Toyama, J. (1999). Amiodarone: Ionic and cellular mechanisms of action of the most promising class III agent. *Am. J. Cardiol.* **84,** 20R–28R.

Komatsu, M., Waguri, S., Koike, M., Sou, Y. S., Ueno, T., Hara, T., Mizushima, N., Iwata, J., Ezaki, J., Murata, S., *et al.* (2007). Homeostatic levels of p62 control cytoplasmic inclusion body formation in autophagy-deficient mice. *Cell* **131,** 1149–1163.

Levine, B., and Klionsky, D. J. (2004). Development by self-digestion: Molecular mechanisms and biological functions of autophagy. *Dev. Cell* **6,** 463–477.

Lullman, H., Lullman-Rauch, R., and Wasserman, O. (1975). Drug induced phospholipidosis. *CRC. Crit. Rev. Toxicol.* **4,** 185–218.

Lum, J. J., Bauer, D. E., Kong, M., Harris, M. H., Li, C., Lindsten, T., and Thompson, C. B. (2005). Growth factor regulation of autophagy and cell survival in the absence of apoptosis. *Cell* **120,** 237–248.

Marchlinski, F. E., Gansler, T. S., Waxman, H. L., and Josephson, M. E. (1982). Amiodarone pulmonary toxicity. *Ann. Intern. Med.* **97,** 839–845.

Martin, W. J., and Howard, D. M. (1985). Amiodarone-induced lung toxicity. In vitro evidence for the direct toxicity of the drug. *Am. J. Pathol.* **120,** 344–350.

Morissette, G., Ammoury, A., Rusu, D., Marguery, M. C., Lodge, R., Poubelle, P. E., and Marceau, F. (2009). Intracellular sequestration of amiodarone: Role of vacuolar ATPase and macroautophagic transition of the resulting vacuolar cytopathology. *Br. J. Pharmacol.* **157,** 1531–1540.

Ni, H. M., Bockus, A., Boggess, N., Jaeschke, H., and Ding, W. X. (2012). Activation of autophagy protects against acetaminophen-induced hepatotoxicity. *Hepatology* **55,** 222–232.

Nicolescu, A. C., Ji, Y., Comeau, J. L., Hill, B. C., Takahashi, T., Brien, J. F., Racz, W. J., and Massey, T. E. (2008). Direct mitochondrial dysfunction precedes reactive oxygen species production in amiodarone-induced toxicity in human peripheral lung epithelial HPL1A cells. *Toxicol. Appl. Pharmacol.* **227,** 370–379.

Ogata, M., Hino, S., Saito, A., Morikawa, K., Kondo, S., Kanemoto, S., Murakami, T., Taniguchi, M., Tanii, I., Yoshinaga, K., *et al.* (2006). Autophagy is activated for cell survival after endoplasmic reticulum stress. *Mol. Cell. Biol.* **26,** 9220–9231.

Paris, I., Muñoz, P., Huenchuguala, S., Couve, E., Sanders, L. H., Greenamyre, J. T., Caviedes, P., and Segura-Aguilar, J. (2011). Autophagy protects against aminochrome-induced cell death in substantia nigra-derived cell line. *Toxicol. Sci.* **121,** 376–388.

Powis, G., Olsen, R., Standing, J. E., Kachel, D., and Martin, W. J., II. (1990). Amiodarone-mediated increase in intracellular free Ca2+ associated with cellular injury to human pulmonary artery endothelial cells. *Toxicol. Appl. Pharmacol.* **103,** 156–164.

Qin, L., Wang, Z., Tao, L., and Wang, Y. (2010). ER stress negatively regulates AKT/TSC/mTOR pathway to enhance autophagy. *Autophagy* **6,** 239–247.

Ramsey, B. W. (1996). Management of pulmonary disease in patients with cystic fibrosis. *N. Engl. J. Med.* **335,** 179–188.

Ravikumar, B., Vacher, C., Berger, Z., Davies, J. E., Luo, S., Oroz, L. G., Scaravilli, F., Easton, D. F., Duden, R., O'Kane, C. J., *et al.* (2004). Inhibition of mTOR induces autophagy and reduces toxicity of polyglutamine expansions in fly and mouse models of Huntington disease. *Nat. Genet.* **36,** 585–595.

Reinhart, P. G., and Gairola, C. G. (1997). Amiodarone-induced pulmonary toxicity in Fischer rats: Release of tumor necrosis factor alpha and transforming growth factor beta by pulmonary alveolar macrophages. *J. Toxicol. Environ. Health* **52,** 353–365.

Reinhart, P. G., Lai, Y. L., and Gairola, C. G. (1996). Amiodarone-induced pulmonary fibrosis in Fischer 344 rats. *Toxicology* **110,** 95–101.

Rogers, D. F. (2003). The airway goblet cell. *Int. J. Biochem. Cell Biol.* **35,** 1–6.

Rosenbluth, J. M., and Pietenpol, J. A. (2009). mTOR regulates autophagy-associated genes downstream of p73. *Autophagy* **5,** 114–116.

Saetta, M., Turato, G., Baraldo, S., Zanin, A., Braccioni, F., Mapp, C. E., Maestrelli, P., Cavallesco, G., Papi, A., and Fabbri, L. M. (2000). Goblet cell hyperplasia and epithelial inflammation in peripheral airways of smokers with both symptoms of chronic bronchitis and chronic airflow limitation. *Am. J. Respir. Crit. Care Med.* **161**(Pt 1), 1016–1021.

Servidddio, G., Bellanti, F., Giudetti, A. M., Gnoni, G. V., Capitanio, N., Tamborra, R., Romano, A. D., Quinto, M., Blonda, M., Vendemiale, G., *et al.* (2011). Mitochondrial oxidative stress and respiratory chain dysfunction account for liver toxicity during amiodarone but not dronedarone administration. *Free Radic. Biol. Med.* **51,** 2234–2242.

Sheppard, M. N., and Harrison, N. K. (1992). New perspectives on basic mechanisms in lung disease. 1. Lung injury, inflammatory mediators, and fibroblast activation in fibrosing alveolitis. *Thorax* **47,** 1064–1074.

Taylor, M. D., Van Dyke, K., Bowman, L. L., Miles, P. R., Hubbs, A. F., Mason, R. J., Shannon, K., and Reasor, M. J. (2000). A characterization of amiodarone-induced pulmonary toxicity in F344 rats and identification of surfactant protein-D as a potential biomarker for the development of the toxicity. *Toxicol. Appl. Pharmacol.* **167,** 182–190.

Tsutsumi, S., Namba, T., Tanaka, K. I., Arai, Y., Ishihara, T., Aburaya, M., Mima, S., Hoshino, T., and Mizushima, T. (2006). Celecoxib upregulates endoplasmic reticulum chaperones that inhibit celecoxib-induced apoptosis in human gastric cells. *Oncogene* **25,** 1018–1029.

Wilson, B. D., and Lippmann, M. L. (1990). Pulmonary accumulation of amiodarone and N-desethylamiodarone. Relationship to the development of pulmonary toxicity. *Am. Rev. Respir. Dis.* **141,** 1553–1558.

Wullschleger, S., Loewith, R., and Hall, M. N. (2006). TOR signaling in growth and metabolism. *Cell* **124,** 471–484.

Yang, M. J., Kim, J. S., Yang, Y. S., Cho, J. W., Choi, S. B., Chung, Y. H., Kim, Y. B., Cho, K. H., Lim, C. W., Kim, C. Y., *et al.* (2008). Pulmonary toxicity and recovery from inhalation of manual metal arc stainless steel welding fume in rats. *Toxicol. Res.* **24,** 119–127.

Yen, Y. T., Yang, H. R., Lo, H. C., Hsieh, Y. C., Tsai, S. C., Hong, C. W., and Hsieh, C. H. (2013). Enhancing autophagy with activated protein C and rapamycin protects against sepsis-induced acute lung injury. *Surgery* **153,** 689–698.

Zhang, H., Kong, X., Kang, J., Su, J., Li, Y., Zhong, J., and Sun, L. (2009). Oxidative stress induces parallel autophagy and mitochondria dysfunction in human glioma U251 cells. *Toxicol. Sci.* **110,** 376–388.

Zhang, T., Qi, Y., Liao, M., Xu, M., Bower, K. A., Frank, J. A., Shen, H. M., Luo, J., Shi, X., and Chen, G. (2012). Autophagy is a cell self-protective mechanism against arsenic-induced cell transformation. *Toxicol. Sci.* **130,** 298–308.